

A silicone-based microfluidic chip grafted with carboxyl functionalized hyperbranched polyglycerols for selective protein capture

Po-Ying Yeh · Nicholas A. A. Rossi ·
Jayachandran N. Kizhakkedathu · Mu Chiao

Received: 7 September 2009 / Accepted: 11 November 2009 / Published online: 25 November 2009
© Springer-Verlag 2009

Abstract A poly(dimethylsiloxane) (PDMS)-based functional microfluidic device containing a charged matrix of PDMS pillar arrays grafted with hyperbranched polyglycerols (HPGs) was developed. Samples of PDMS were modified with allylamine plasma to form amine groups on the surface prior to the covalent grafting of succinimide ester-functionalized HPGs. The anionic functionality of the PDMS channel matrices was developed by altering the number of carboxyl groups present on the HPGs. The grafting of HPGs onto PDMS plates was investigated via contact angle measurement and attenuated total reflectance-Fourier transform infrared spectroscopy (ATR-FTIR), while the grafting of the inside channel was investigated by electroosmotic flow (EOF) measurements. The charge density on grafted HPG was optimized to minimize the nonspecific protein adsorption and increase the selective capture of positively charged proteins. A proof-of-concept device was fabricated on PDMS and demonstrated that the device selectively captures positively charged protein (avidin) from a mixture of bovine serum albumin (BSA)-avidin at pH 7.4 in phosphate buffered saline (PBS). In order to increase the capture efficiency of the proteins in this PDMS-based device, pillar arrays have been fabricated within the channel. As a demonstration, the new device separated two proteins with an avidin capture

efficiency of $100 \pm 2.95\%$ per 3 min from a 0.02 mg/ml protein solution (avidin:BSA wt ratio: 1:1). This new microfluidic-based device shows a great deal of promise as a tool for protein capture and analysis.

Keywords PDMS microfluidic devices · Protein separation · Nonfouling · Hyperbranched polyglycerols

1 Introduction

Recent developments in microfluidic systems have provided important platforms for biomedical applications such as liquid chromatography (LC) (He et al. 1998; Lazar et al. 2006; de Malsche et al. 2007), proteome profiling (Ramsey et al. 2003; Wang et al. 2004; Thongboonkerd et al. 2007), cell sorting (Yao et al. 2004), and biochemical analysis (Burns et al. 1998). Microfluidic systems use microfabricated channels that are easy to fabricate and have the advantages of reagent reduction and increased accuracy (Kim et al. 2006). Poly(dimethylsiloxane) (PDMS) is one of the most popular materials used in microfluidic devices due to its low cost and easy fabrication. PDMS is highly resistant to chemicals and can be bonded to glass and other polymeric materials using appropriate surface treatments. However, PDMS is highly hydrophobic, and the hydrophobic interactions between PDMS surfaces and biologic reagents, such as DNA and proteins, can cause reagent loss and subsequent biofouling (Effenhauser et al. 1997; Bi et al. 2006; Muck and Svatos 2007; Xiao et al. 2007). When manipulating small quantities of reagents, any loss of the sample and surface biofouling will cause critical errors and malfunction of the device. For biologic analysis, it is paramount that the surface fulfills certain criteria, such

P.-Y. Yeh · M. Chiao (✉)
Department of Mechanical Engineering, University of British
Columbia, Vancouver, BC, Canada
e-mail: muchiao@mech.ubc.ca

N. A. A. Rossi · J. N. Kizhakkedathu (✉)
Department of Pathology and Laboratory Medicine, Centre for
Blood Research, University of British Columbia, Vancouver,
BC, Canada
e-mail: jay@pathology.ubc.ca

as wettability, compatibility with bio-fluids, and resistance to nonspecific adsorption. Furthermore, when biologic reagents adsorb onto the PDMS surface, the electrical double layer will be perturbed by the charged analytes, leading to heterogeneous zeta potentials present on the PDMS surface. Since the velocity of electroosmotic flow (EOF) depends on the zeta potential (Liu and Lee 2006), a nonuniform EOF will be generated, causing analytical irreproducibility and poor resolution for biochemical analysis and electrophoresis.

Recently, different surface modification approaches have been applied to PDMS microfluidic channels to increase surface hydrophilicity and reduce reagent adsorption to stabilize the EOF. Among the reported techniques, embedding (Huang et al. 2006; Yu and Han 2006) and grafting (Wu et al. 2006; Guo et al. 2007) of polymer “brushes” onto PDMS surfaces are popular methods for permanent surface modification. In these cases, the polymers must contain hydrophilic chains, similar interfacial free energies compared to water, and large degrees of mobility (Norde et al. 2005). In the case of neutral hydrophilic polymer brushes, the steric barrier, caused by high conformational entropy of the anchored chains, is the main contributing factor toward attenuation of nonspecific adsorption (McNamee et al. 2007; Satulovsky et al. 2007; Singh et al. 2007). Several factors, including pH, molecular weight, and grafting density of the polymer chain conformation, may affect the final performance of polymer-coated microfluidic channels (Hu et al. 2002; Thormanna et al. 2007; Wang et al. 2007).

One of the commonly used antifouling polymers is poly(ethylene glycol) (PEG) (Harris 1992; Cima 1994; Tessmar and Göpferich 2007). The main disadvantage of PEG is its susceptibility to oxidation and subsequent degradation (Sharma et al. 2003). Moreover, PEG has limited functionality due to its linear nature. When anchored at one end, the surface density and functionality decreases with increasing molecular weight (Milner 1991). In order to reduce nonspecific adsorption, issues associated with limited functionality may not be as important as other parameters. However, for the development of functional surfaces for devices such as biosensors and protein separation instruments, a decrease in surface functionality is a major disadvantage. Therefore, the development of a dual purpose surface, which not only reduces nonspecific adsorption but also imparts chemical functionality, is of great interest to the field of microfluidics (Stadler et al. 2007).

The use of dendritic or hyperbranched polymers with multiple peripheral functional groups has gained significant attention in recent years. It has been demonstrated that such polymers can be modified with a broad range of functional groups and biomolecules, such as peptides, antibodies, and

DNA, for various biomedical applications (Pathak et al. 2004; Ajikumar et al. 2007). Recently, our group showed that hyperbranched polyglycerols (HPGs) are highly biocompatible, resistant to protein nonspecific adsorption, and can be functionalized to various degrees due to the presence of large amount of reactive hydroxyl groups (Kainthan et al. 2006a; 2008; Yeh et al. 2008; Zhang et al. 2008). As a result, grafting HPGs to materials surface will likely result in a functional and nonfouling interface. It is also important to note that, unlike dendrimers, HPGs can be easily synthesized in significant quantities and with good control over polymer properties (Kainthan et al. 2006b).

Here, the use of the ion-exchange concept in a microchannel column for efficient protein capture and separation is reported (Fig. 1). Surface grafted HPG was used both as a specific protein capture agent as well as a layer to prevent nonspecific protein adsorption onto the PDMS surface. The microchannel columns were fabricated on PDMS with uniform pillar arrays; the channel surfaces were modified using a functional HPG for capture and release of biologic reagents, while the nonspecific adsorption was significantly reduced.

2 Materials and methods

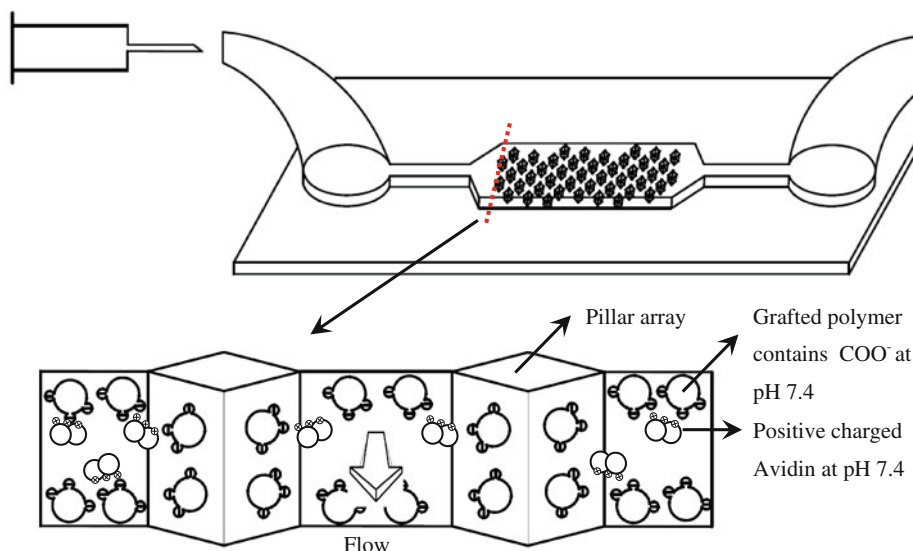
2.1 Materials

Bovine serum albumin-fluorescein isothiocyanate (BSA-FITC, A9771) and avidin-Rhodamine conjugate (R01) were purchased from Sigma–Aldrich Corp. and Biomedica Corp., respectively, and used without further purification. Phosphate buffered saline (PBS) has a concentration of 0.067M PO_4 and 0.15M NaCl. Inorganic salts were purchased from Fisher Scientific except $\text{NaH}_2\text{PO}_3 \cdot \text{H}_2\text{O}$ which was procured from EMD Bioscience Inc. RTV 615 polydimethylsiloxane (PDMS) prepolymer and curing agent were purchased from GE Silicones. All other reagents for the synthesis and modification were purchased from Aldrich Chemical Corp.

2.2 Microfabrication

The PDMS prepolymer (RTV 615A) was mixed thoroughly with a curing agent (RTV 615B) at 10:1 (v/v) and degassed with a vacuum pump. PDMS microchannels were fabricated using soft lithography (Xia and Whitesides 1998). A photosensitive polymer, SU8 2025 (NanoTM SU8-2025, Microchem), was patterned by a conventional lithography tool (UV 405 nm, Canon mask aligner). The height of SU8 mold on the silicon substrate was 30 μm after spinning at 3000 rpm for 30 s and baked using the following protocol: SB (soft bake): 65°C for 2 min, and

Fig. 1 Illustration of a PDMS based microfluidic device for the selective capture of relevant proteins



95°C for 5 min; PEB (postexposure bake): 65°C for 1 min, and 95°C for 3 min. The lithography mask was designed by L-edit™ (Tanner Research, Inc.) and printed on a transparency sheet (Output City CAD/Art Services, Inc.) with a resolution of 20,000 dpi and minimum feature size of 10 μm. The microchannel cover was a glass slide coated with PDMS spun at 1000 rpm for 1 min. The PDMS solution was poured over the SU-8 mold. Both the PDMS microchannel and the cover were cured at 80°C for 1 h. After peeling off from the SU-8 mold, holes with a diameter of 1.2 mm were mechanically punched as inlet and outlet of device on the PDMS microchannel. The PDMS microchannel and cover were bonded by O₂ plasma treatment (150 W, 300 mTorr, 10 s, Trion PECVD) under finger pressure.

2.3 Polymer synthesis and grafting protocol

Hyperbranched polyglycerol was synthesized from glycidol according to published procedures (Kainthan et al. 2006b). Functionalized polyglycerols containing reactive succinimidyl ester groups were synthesized according to methods published previously (Rossi et al. 2008). Different carboxyl functionalized HPGs were synthesized by changing the molecular weight of HPG and number of carboxyl groups per HPG (Table 1).

PDMS plates were used initially for developing surface modification protocol, which was later adapted for microchannel modification. PDMS surfaces were treated with plasma in a M4L plasma reactor (PVA TePla Corp.) before polymer grafting. The plasma power was delivered at 13.56 MHz. PDMS plates and devices were treated using the following protocol: Ar plasma of 75 W, 50 sccm, 350 mTorr for 1 min, and allylamine plasma at 55 W, 80 sccm,

540 mTorr for 10 min. The optimization of allylamine plasma modification was described in the supporting information. After plasma treatment, the modified surfaces were washed with soap, water, methanol, and Mili-Q water (Millipore, Inc.) and were stored in Mili-Q water until polymer grafting.

Synthesized polymers were dissolved in Mili-Q water just before contacting the PDMS surfaces. The concentration of each polymer solution used was 1.4 mg/ml. PDMS surfaces were immersed in polymer solution for 1 h without stirring. For the microchannels, the polymer solutions (1.4 or 3 mg/ml) were injected into microchannels every 10 min for 1 h. After reaction, the surfaces were sonicated in Mili-Q water for 10 min and then flushed with water to remove unattached polymer from surfaces. The surfaces were treated with allylamine plasma (NH₂) and grafted with HPG-P1 (2.5 kDa), HPG-P2 (8 kDa), and HPG-P3 (8 kDa, 5–6 COOH groups per molecule).

2.4 Contact angle measurements

The static contact angles of untreated and the surface-modified PDMS plates were measured by a sessile drop contact angle apparatus (Meulchen Mark I). A 30 μl drop of Mili-Q water was placed on the surface of PDMS plates,

Table 1 The properties of HPGs and number of COOH groups after grafting to PDMS surfaces

	Molecular weight (g/mole)	Number of active succinimidyl ester groups	Number of remaining acid groups
HPG-P1	2,500	3	0–1
HPG-P2	8,000	5	2–3
HPG-P3	8,000	8	5–6

and then the images were taken. The water contact angles on PDMS plates were measured at least eight places, and the average value is reported.

2.5 FTIR measurements

ATR-FTIR absorption spectra were collected using a Nexus 670 FT-IR ESP (Nicolet Instrument Corp., Waltham, MA) with an MCT/A liquid nitrogen-cooled detector, KBr beam splitter, and a MkII Auen Gate Single Reflection attenuated total reflectance (ATR) accessory (Specac Inc., Woodstock, GA). The sample stage contains a diamond window and a sapphire anvil on a torque limiting screw set to deliver 80 lbs. of pressure. IR spectra of the surfaces were recorded from 800 to 4000 cm^{-1} at room temperature.

2.6 Electroosmotic flow (EOF) measurements

The PDMS microchannel was filled with PBS buffer for at least 3 h before EOF measurement. The voltage was applied on two ends of the microchannel filled with buffer, and the velocity of flow was measured for four channels, plasma-oxidized, NH_2 -, HPG-P2-, and HPG-P3-grafted PDMS.

2.7 Nonspecific protein adsorption

The PDMS plates were incubated and the microchannels were filled initially with PBS buffer for at least 3 h and then with 2 mg/ml BSA in PBS buffer at room temperature for 1 h to evaluate the performance of attenuation of nonspecific protein adsorption.

Following incubation, the surfaces were rinsed thoroughly with PBS to remove loosely adsorbed proteins (PDMS plates were washed 5 times, while microchannels were injected with PBS 3 times). Fluorescent images of the PDMS surfaces were taken by a fluorescence microscope (Nikon eclipse TE 2000-U with X-Cite 120 fluorescence illumination system, fluorescein isothiocyanate (FITC) filter, and DS-U1 suit digital camera). The amount of adsorbed BSA is linearly related to the fluorescence intensity (Stadler et al. 2007). The fluorescence intensity was analyzed by Adobe PhotoshopTM 6.0. The relative fluorescent intensity on the surface was normalized by a calibration scale in which the intensity of untreated PDMS surface without protein was set to 0%, and the intensity of protein exposed untreated PDMS surface was set to 100%.

2.8 Selective protein capture and separation in microchannels

The PDMS microfluidic devices with pillar arrays were incubated with 1 mg/ml BSA, or 1 mg/ml avidin solutions, or avidin-BSA mixtures (wt ratio: 1:1) of 0.2, 0.066,

0.02 mg/ml at room temperature for 3 min to evaluate the capture efficiency. The microchannel surfaces were then washed by injecting PBS 3 times into the channel.

The BSA was labeled with FITC, while avidin was labeled with Rhodamine Red. The fluorescent images of the protein adsorbed surfaces were taken by a fluorescence microscope as with a DAPI (4'-6-Diamidino-2-phenylindole)-FITC-TRITC (Tetramethyl Rhodamine Isothiocyanate) filter. The images were taken in RGB mode, and then split into three separate color channels (red, green, and blue). However, the overlapping emission spectra of FITC and Rhodamine Red (Rh) caused the spectra cross talk between color channels, which reduced resolvability (Chen et al. 2005). The reason of cross talk is due to the emission spectra of most fluorescence dyes are broad and have long tails. Hence, the green (red) color seen in Photoshop is mainly from FITC (Rh) and partially from Rh (FITC). For better protein quantification through fluorescence measurement, this issue needs to be addressed and compensated. The first step is to measure pure-labeled BSA and avidin solution separately. It was found that the color intensity ratios of green/red and red/green color of Rh-avidin and FITC-BSA are 0.427 and 0.227 (average from four images), respectively. Hence, if the red and green intensities contributed from avidin and BSA are taken as x and y , respectively, then the total red and green intensities seen in Photoshop are actually $x + 0.227y$ and $y + 0.427x$, respectively (the quantity ratio of avidin/BSA mixture is 1). The parameters x and y can be calculated from the measured green and red intensities (2 unknown and 2 equations) of specific conditions (before (x, y) and after 3 min incubation in protein solution (x', y')).

The performance of the protein capture column was evaluated by measuring the capture efficiency (% per 3 min) and the protein present in output (avidin or BSA). The capture efficiency, E_a and E_b for avidin and BSA, was defined as the relative percentage of capture per 3 min (%), $x'/x \times 100$ and $y'/y \times 100$). It is noted that although the parameters x and y are not quantitative enough for the concentration calculation, they are related to the quantities of avidin and BSA. The avidin in the outlet is calculated from the total amount and the captured amount in the channel, which is $C_a \times V - (x'/x) \times C_a \times V$. Also, output quantity of BSA is $C_b \times V - (y'/y) \times C_b \times V$, where V is the volume of the channel, C_a and C_b are the injected concentration of avidin and BSA, respectively. The percentage of avidin in the outlet over the protein mixture is hence $100\% \times (C_a \times V - (x'/x) \times C_a \times V) / ((C_a \times V - (x'/x) \times C_a \times V) + (C_b \times V - (y'/y) \times C_b \times V))$, which equals $100\% \times (100 - E_a)C_a / ((100 - E_a)C_a + (100 - E_b)C_b)$. The percentage of BSA in the outlet over the protein mixture is $100\% \times (100 - E_b)C_b / ((100 - E_a)C_a + (100 - E_b)C_b)$.

2.9 Optical profiler

A Wyko NT1100 Optical Profiling System uses interferometry to measure surface profiles. The SU8 mold was focused under a 20× objective lens. The silicon substrate was the focus plane and the height and topography were constructed by a back scan of 40 μm, and the stage tilt was compensated by software.

2.10 Scanning electron microscope (SEM)

Surfaces were imaged using a Hitachi S-3000N scanning electron microscope with a tungsten electron source. The accelerating voltage can be varied over the range of 0.5–30 kV. The device was glued on a carbon stick and coated with a thin gold by a plasma generator. A conductive carbon paste was connecting the gold film to the bottom of the carbon stick for reducing electron accumulation.

3 Results and discussion

3.1 Polymer coating and validation

Functional surfaces with controlled properties have attracted substantial research interest recently. Potential applications include self-cleaning surfaces (Wang et al. 1997), devices of intelligent interfaces for biologic separation (Mu et al. 2007) and assays (electrophoresis-based (He et al. 1998) and pressure-based chromatography (Lazar et al. 2006; de Malsche et al. 2007)), and tissue engineering (Shimizu et al. 2001). In this study, HPG was used as scaffold for creating functional and nonfouling surfaces in microfluidic channels.

HPG was functionalized with succinimidyl ester groups by reacting a fraction of the available hydroxyl groups (for example, HPG 8k contains approximately 100 available OH groups) with succinic anhydride (Rossi et al. 2008). The structure of succinimidyl ester-functionalized HPG is shown in Fig. 2a. The succinimidyl ester groups hydrolyze in water to form N-hydroxysuccinimide and carboxylic acids (half-life of succinimidyl ester groups in water is ~16 min) (Roberts et al. 2002). Hence, the number of acid groups generated on the surface of the HPG after degradation of succinimidyl ester groups was varied by using different molar ratios of OH groups to succinic anhydride. For example, with a molar ratio of 1:5, each HPG should theoretically have an average of 5 acid groups. The succinimidyl ester groups on the surface of HPG is also as the reactive group to react with the amino groups on the surface of PDMS.

Initially PDMS plates were used as a model surface to optimize the grafting protocol prior to the use of similar

strategies to modify PDMS microchannels. This is due to the convenience of following the surface modification on a flat surface compared to microchannels (contact angle and FT-IR measurements are possible in the former case). Argon plasma treatment before allylamine plasma treatment was necessary for efficient amine modification. These amine functionalized PDMS surfaces and microchannels were reacted with succinimidyl ester-modified HPG to generate a HPG-grafted surface. The reaction scheme is shown in Fig. 2b. Any remaining unreacted succinimidyl ester groups present on the grafted HPGs will be hydrolyzed to carboxyl acid groups. This process generated a covalently coupled, anionic polymer layer in PBS buffer at pH 7.4 on the microchannel walls, as well as PDMS plates. The properties of the different HPGs, namely molecular weight, number of active succinimidyl ester groups, and number of carboxyl groups, are listed in Table 1.

Water contact angles of the PDMS plates were measured and are shown in Fig. 3a. They were $100.4 \pm 4.4^\circ$, $89.2 \pm 1.8^\circ$, $80.6 \pm 3.5^\circ$, $73.2 \pm 2.8^\circ$, and $77.6 \pm 1.2^\circ$ for untreated, NH₂-modified, HPG-P1-, HPG-P2-, and HPG-P3-grafted PDMS surfaces, respectively. After plasma treatment, the surface became less hydrophobic due to the incorporation of more hydrophilic amine groups, as highlighted by the lower water contact angle. Upon HPG grafting, the PDMS surface became relatively hydrophilic due to the formation of a prewetting water layer on the HPG caused by hydrogen bonding (Prime and Whitesides

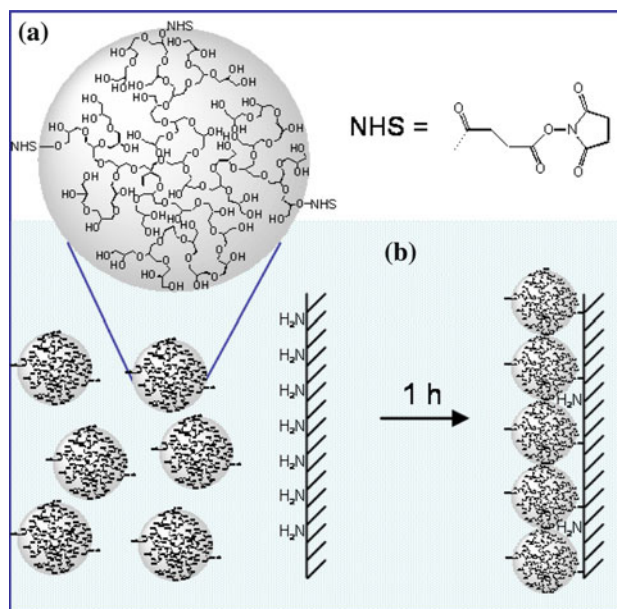


Fig. 2 *a* Representation of the chemical structure of HPG containing functional succinimidyl ester groups (molecular weights 2.5 or 8 kDa) and *b* the reaction scheme involving the grafting process of functionalized HPG to amine modified PDMS surfaces

1993; Xiao et al. 2002). A slight increase in the water contact angle for HPG-P3-grafted surface compared to HPG-P2 may due to the presence of more amount of less hydrophilic carboxyl groups connected via ester on HPG-P3. This observation is supported by the reports by Barbosa et al. (2005) and Martin et al. (2003) that the water contact angles of surfaces grafted with OH terminal polymers were lower than the corresponding COOH terminal polymer. The difference between HPG-P1 and HPG-P2 is due the difference in the molecular weight of the polymer. Higher molecular weight gave lower contact angle presumably due to the better surface coverage.

The surface modification was further investigated by ATR-FTIR spectroscopy. As shown in Fig. 3b, verification of HPG grafting on the PDMS plate is evidenced by characteristic C–O–C stretching around 1100 cm^{-1} , C–H stretching at 2875 cm^{-1} , and a small broad peak around 3400 cm^{-1} due to hydroxyl stretching of HPG (Yeh et al. 2008). Similar ATR-FTIR profiles were shown when different HPG preparation was used for surface modification (Fig. 3b). The current grafting method was also compared with other grafting chemistries such as the use of aldehyde chemistry; results are described in the supporting

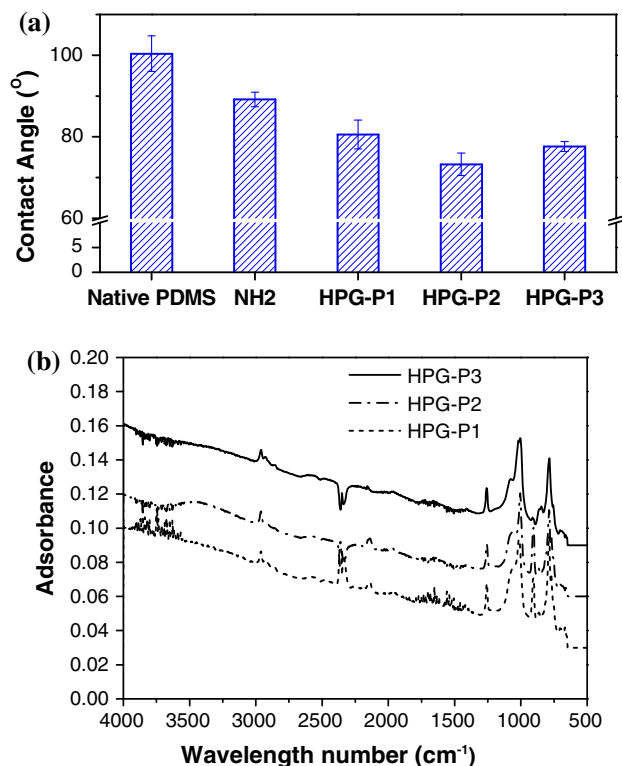


Fig. 3 **a** Contact angles of untreated, amino (NH_2), HPG-P1, HPG-P2, and HPG-P3 modified PDMS surfaces (error bars extrapolated from standard deviations from total of 8 measurements), and **b** FTIR spectra of HPG-P1, HPG-P2, and HPG-P3 modified PDMS surfaces. The surfaces were dried before contact angle and FTIR measurements

information. The current method produced maximum HPG grafting on the PDMS surface.

In order to verify HPG grafting and the presence of carboxylic acid groups within the PDMS microchannels, electroosmotic flow (EOF) measurements were performed for plasma-oxidized, NH_2 -modified, HPG-P2-, and HPG-P3-grafted microchannels. The mobility of EOF (μ_{EOF}) is defined as $V_{\text{EOF}} \times E^{-1}$, where V_{EOF} and E are the velocity and electric field, respectively (Squires and Quake 2005). E is equal to the applied voltage divided by the distance between the electrodes ($E = 4 \times 10^3$ for plasma-oxidized and 16×10^3 V/m for HPG-P2-, HPG-P3-, NH_2 -modified microchannels). The difference in applied electric field of amine-modified channels is due to the shorter length of the channel. However, this difference will not affect the conclusions. Alternatively, μ_{EOF} can be defined as $\varepsilon\zeta/\eta$, where ε and η are the permittivity and viscosity of the solution, respectively; ζ is the zeta potential which depends linearly on the surface charge density (Xiao et al. 2002). Since all the measurements were performed in PBS buffer, variations in the velocity of EOF in the PDMS microchannels can only be due to the different surface treatments and changes in the zeta potential. A comparison of the EOF mobilities measured for plasma-oxidized, NH_2 , HPG-P2, and HPG-P3-grafted microchannels are shown in Fig. 4. The μ_{EOF} measured for the plasma oxidized PDMS microchannel after O_2 plasma treatment is $3.84 \pm 0.16 \times 10^{-4} \text{ cm}^2/\text{V s}$ (mobility is a vector which has the same direction as electric field). The value of EOF velocity shows that the PDMS surface is negatively charged; this can be correlated to the formation of silanol groups or carboxyl groups produced during O_2 plasma treatment. The μ_{EOF} of the NH_2 -modified PDMS microchannel is $-0.86 \pm 0.29 \times 10^{-4} \text{ cm}^2/\text{V s}$. The NH_2 -modified surface poses a net positive charge and hence the direction of EOF is reversed compared to the O_2 plasma-treated PDMS surface. The HPG-P2-grafted microchannel has a mobility of $1.6 \pm 0.52 \times 10^{-4} \text{ cm}^2/\text{V s}$. The complete reversal of mobility compared to the amine-treated surface is further evidence for the presence of grafted HPG-P2 in the microchannel. For HPG-P3 grafted microchannels, the value of EOF ($4.19 \pm 0.07 \times 10^{-4} \text{ cm}^2/\text{V s}$) increased compared to HPG-P2-grafted channels. This is due to the presence of a higher percentage of peripheral carboxylic acid groups on HPG-P3 (see Table 1), which causes a higher zeta potential closer to the surface. The higher water contact angle of HPG-P3-grafted surface given earlier also supports this observation.

3.2 Nonspecific protein adsorption reduction

Nonspecific protein adsorption onto both the PDMS plates and microchannels was investigated using FITC-labeled

BSA. The relative fluorescence intensities of FITC-BSA-incubated PDMS plates and microchannels are shown in Fig. 5a; the values for NH₂-modified, HPG-P1-, HPG-P2-, and HPG-P3-grafted PDMS surfaces compared to the native PDMS (untreated PDMS in the case of plates and plasma-oxidized PDMS in the case of PDMS microchannels) surface decreased ~1.25, 2.77, 3.7, and 3.33-fold, respectively. The higher hydrophilicity of NH₂-modified surface may have caused a reduction in BSA adsorption to this surface. Furthermore, surfaces grafted with HPGs strongly attenuated the BSA adsorption. However, there were no significant differences between the relative fluorescent intensities on surfaces grafted with different HPG preparations. In the case of the microchannels, the fluorescent intensities decreased to ~1.55, 4.16, 4.16, 5.88-fold, respectively, for NH₂ modified, HPG-P1, HPG-P2, and HPG-P3 (Fig. 5b) compared to control channels. Although HPG-P3 has more carboxyl groups present, it did not show any significant change in nonspecific protein adsorption suggesting that a functional and nonfouling surface is produced on PDMS plates and in the microchannels. The only difference between HPG-P2 and HPG-P3 modification is the presence of additional carboxyl groups on HPG.

3.3 Selective protein capture

Having grafted a nonfouling and functional polymer layer to the microchannels, the potential application of this coating as an ion-exchange liquid chromatographic material is tested. The concept (Fig. 1) involves the use of a PDMS ion exchange column grafted with HPG to selectively capture a specific reagent from a mixture. The inlet and outlet are connected to a syringe to generate a fluid

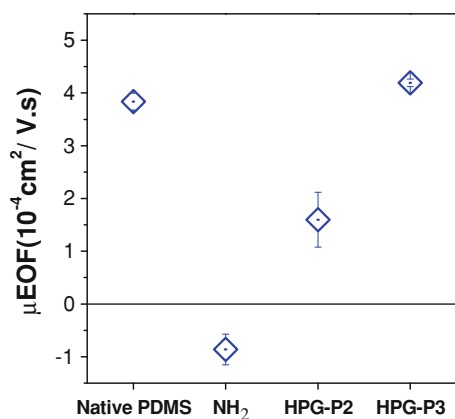


Fig. 4 Values of measured μ_{EOF} of plasma-oxidized, amino (NH₂), HPG-P2-, and HPG-P3-modified PDMS microchannels. The applied electric fields for plasma-oxidized, HPG-P2-, and HPG-P3-modified microchannels are 4×10^3 V/m. The applied electric field for amino-modified microchannels is 16×10^3 V/m. The average velocity and error bars are from three independent measurements

flow. Polymer coatings with negatively charged stationary phases are used to capture positively charged proteins, and vice versa. The microfluidic device comprises 300 μm wide channels, connecting an inlet and outlet to a separating column (1350 μm wide and 5000 μm long). The topography of the SU8 mold was profiled by an optical profiler (Fig. 6a). The height of the SU8 pillar mold is around 30 μm. The SEM images of the PDMS replica peeled off from the SU8 mold are shown in Figs. 6b and c. Although the heights of the PDMS channel walls and pillars should be around 30 μm, the cross section of PDMS pillar as measured by SEM after curing is approximately 15 μm × 15 μm due to lithography error and shrinking of the PDMS after curing (the cross section in mask design is 20 μm × 20 μm). The surface area-to-volume ratio of this column design with pillar arrays was 0.11 (1/μm) compared to 0.066 for those without pillar arrays, corresponding to an increase of ~67%. A further increase in this ratio can be made possible by using molds with higher stationary phase densities and lower aspect ratios (i.e., by lowering the height of the channel). The effective volume and surface area of the current column are 1.7415×10^{-4} cm³ (5000 μm × 1350 μm × 30 μm × ((40² - 15²)/40²)) and 1.9514×10^{-1} cm², respectively.

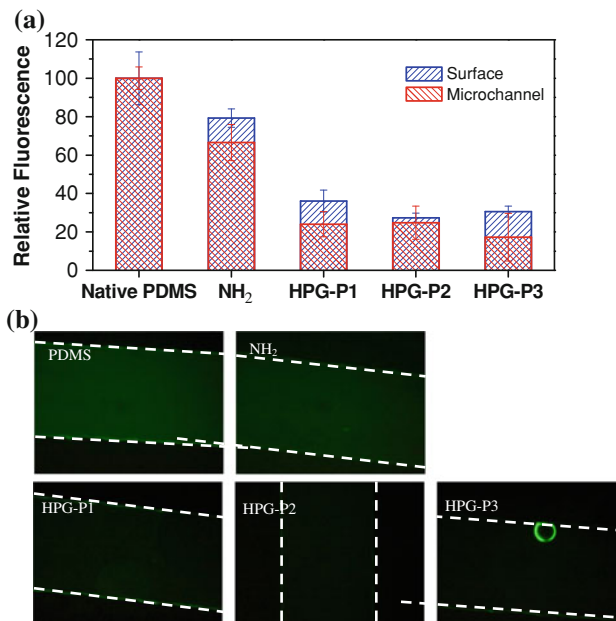


Fig. 5 a Fluorescence intensities of native (untreated PDMS for plates and plasma-oxidized PDMS for PDMS microchannels), amino (NH₂), HPG-P1, HPG-P2, and HPG-P3 modified PDMS surfaces and microchannels after FITC-labeled BSA adsorption (the error bars in the figure are the standard deviation of six measured data points). The BSA solution was incubated with PDMS surfaces for 1 h at room temperature. After adsorption, PDMS surfaces and microchannels were washed with PBS buffer 5 and 3 times, respectively. **b** Fluorescence photos of the plasma-oxidized, amino (NH₂-), HPG-P1-, HPG-P2-, and HPG-P3-modified PDMS microchannels shown in a. The white dash lines are the boundaries of the microchannels

Two proteins, BSA and avidin, are used as model proteins for the separation experiments since they are negatively and positively charged, respectively, in PBS, pH 7.4 (isoelectric points (IP) of BSA and avidin are 4.7 – 5.0 (de Vasconcelos et al. 2007) and 10.5 (Mu et al. 2007), respectively). The HPG-P3-grafted channels were filled with a solution of proteins at a concentration of 1 mg/ml and washed after 3 min. Fluorescent images of channels filled with 1 mg/ml avidin and BSA are shown in Fig. 7a and c. Fluorescence images of channels incubated with 1 mg/ml avidin and BSA for 3 min and then washed 3 times with PBS buffer are shown in Fig. 7b and d. The relative fluorescent intensity of Fig. 7b is $21.17 \pm 2.78\%$ of Fig. 7a, and the relative fluorescent intensity of Fig. 7d is $8.84 \pm 1.23\%$ of Fig. 7c. This suggests that there is a preference for the absorption of positively charged avidin compared to negatively charged BSA to this channel under the conditions used. The relatively low capture efficiency from a high concentration protein solution might be due to the saturation of protein adsorption at a given incubation time caused by a high concentration of proteins. Hence, lower concentrations (0.02, 0.066, 0.2 mg/ml, wt: 1:1) of the protein mixtures were employed to further evaluate the column selectivity.

Fluorescence images of the column at the start of the experiment at 0.2 mg/ml total protein concentration (0.1 mg/ml of avidin and BSA each) and the end of the experiment (3 min incubation and washing) are shown in Fig. 8a and b, respectively. The fluorescence intensity ratio of red/green at the onset of filling of the protein mixture (0.96, which is 46.55/48.54), followed by a 3 min incubation period and washing 3 times with PBS (2.36, which is 22.20/9.42) is shown in Fig. 8c. There is a marked difference in the color (green–red) of the column after protein mixture incubation and washing, indicating that more avidin was adsorbed from the protein mixture compared to BSA. The quantities of avidin and BSA were calculated as the methods described before. Assuming the red and green intensities of avidin and BSA are x and y , respectively. The red and green intensities measured by Photoshop are actually $x + 0.227y$ and $y + 0.427x$, respectively. The average (four images) red and green intensities observed in

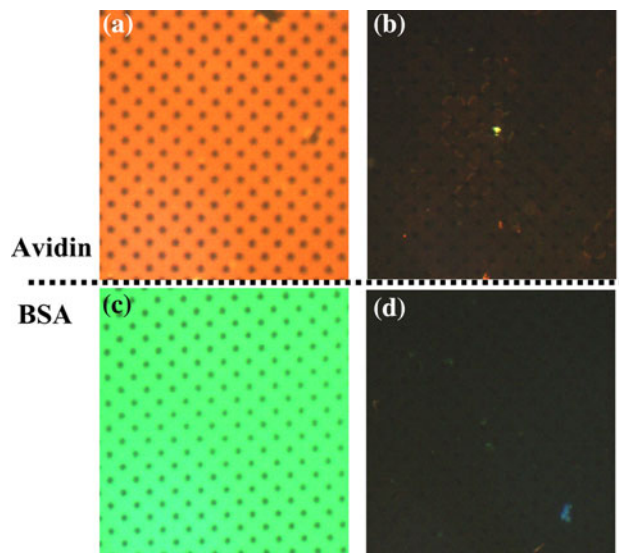


Fig. 7 Fluorescence images of columns **a** filled with avidin, **b** incubated with avidin for 3 min and washed 3 times with PBS buffer (the fluorescent intensity decreased 4.76-fold compared to **a**), **c** filled with BSA, **d** incubated with BSA for 3 min and washed 3 times with PBS buffer (the fluorescent intensity decreased 11.3-fold compared to **c**). The concentration of BSA and avidin was 1 mg/ml, and the measurement was performed at room temperature. The fluorescence microscopic images shown were further processed by Word™ to increase the contrast and brightness of photos. However, the original images were used to measure the fluorescent intensity

Fig. 8a are 46.55 and 48.54, respectively. Hence, the x and y are 39.34 ± 1.0 and 31.75 ± 4.4 , respectively. A similar calculation was applied on the Fig. 8b to yield x' and y' as 22.2 ± 0.62 and $\sim 0 \pm 2.74$, respectively. With the assumption that the color intensity is linear related to the protein quantity and the quantity ratio of avidin to BSA is 1, the relative quantities of avidin and BSA in Fig. 8a and b can be evaluated. After 3 min incubation and 3 times PBS washing, 56.4% ($22.2/39.34 \times 100\%$) of avidin was captured by the device. The quantity y' is close to 0, however, due to the variation of single color fluorescence intensity and two color fluorescence overlap; this compensated y' should be considered a relatively small quantity compared to y rather absolute 0.

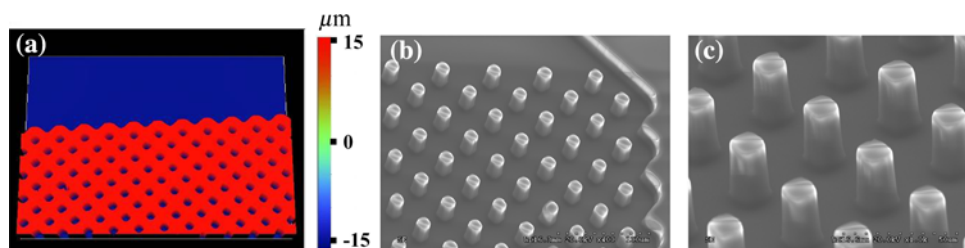
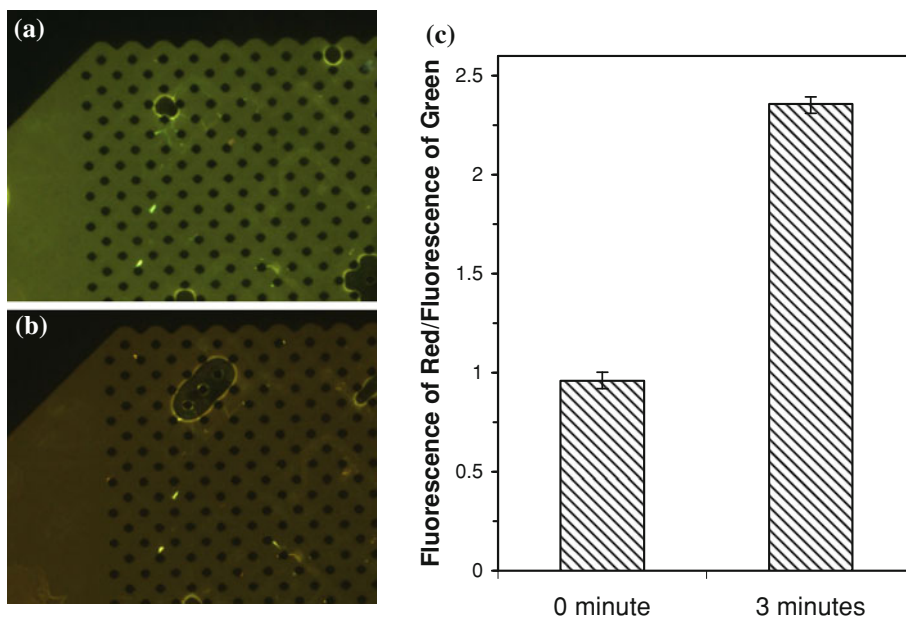


Fig. 6 **a** The topography SU8 mold on a silicon substrate measured by an optical profiler (part of the ion exchange column, scale is shown in the figure). The SEM photos of **b** $\times 400$, and **c** $\times 1000$ PDMS pillar

arrays. The dimensions of the cross section of the pillar arrays are $15 \mu\text{m} \times 15 \mu\text{m}$

Fig. 8 Fluorescence images of columns at **a** 0 min after incubation with protein mixture (0.1 mg/ml avidin and 0.1 mg/ml BSA), **b** After 3 min incubation and 3 times wash with PBS buffer and **c** fluorescence intensity ratio of red/green at the onset and after 3 min of incubation (followed by washing 3 times with PBS buffer) with the protein mixture (error bars extrapolated from standard deviations from total of 6 measurements)



The selectivity based on the percentages of relative amount of protein is almost the infinite since very few BSA remained after PBS washing. The high selectivity of avidin indicates that the HPG layer considerably prevented non-specific adsorption, while enhancing specific protein binding by electrostatic interaction. The capture efficiency of the column upon filling with a 0.2 mg/ml (wt: 1:1) protein solution is 56.4% after 3 min. The captured avidin was also released using a higher ionic strength buffer solution (10 times Na⁺ ion strength). After 3 times 10× PBS washing, ~45.5% of captured avidin was released from the column.

The column performance upon incubation with lower concentrations of the protein mixtures (0.066 and 0.02 mg/ml) was also investigated. With decreasing protein concentration (from 0.2 to 0.02 mg/ml), the capture efficiency of avidin increased up to ~100%. In order to confirm the selective capture of avidin by the HPG-P3 layer, a control experiment was performed using a HPG-P2-grafted column. The experiment described above was repeated using a 0.02 mg/ml avidin–BSA (1:1) mixture. It was found that the percentages of avidin and BSA present in the column after PBS washing were 64.6 and 53.6%, respectively, with a ratio of avidin/BSA of 1.1. In contrast to the HPG-P3-grafted layer, HPG-P2 did not show any preference for proteins.

The residual protein adsorption observed here may be due to the nonspecific adsorption of protein, which was minimized but not completely eliminated. In light of our previous experiments (Yeh et al. 2008), the grafting density of HPG-P3 inside the microchannels was increased to investigate column performance by increasing the HPG incubation concentration (3 mg/ml instead of 1.4 mg/ml). The avidin capture efficiency and ratio of avidin/BSA of the column upon incubation with 0.066 and 0.020 mg/ml

avidin–BSA mixtures were 76.4% & 4.5, and ~100% & 10.9, respectively. Increasing the polymer graft density did not produce any observed improvement in column performance in the current setting. However, an increase in polymer density did produce a decrease in nonspecific BSA adsorption (data not shown). It is important to note that the functional characteristics of the polymer coatings can be optimized to achieve maximum selectivity and minimum nonspecific adsorption.

The percentage of avidin or BSA in the outlet of channels after being passed through the channels is shown in Fig. 9. For a given protein mixture concentration (0.066 mg/ml), the capture efficiency of avidin and BSA was 86.8 and

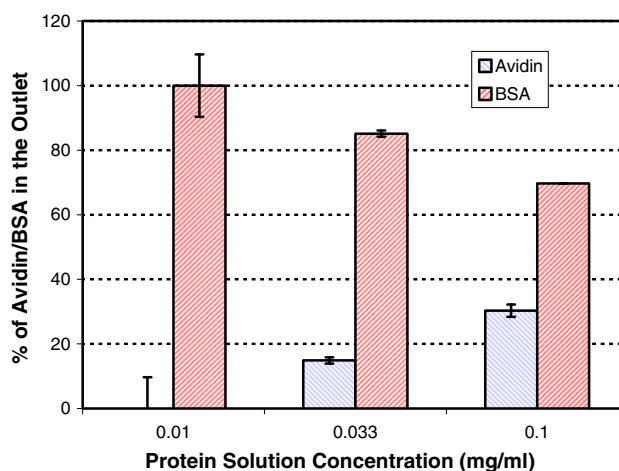


Fig. 9 The percentage of avidin or BSA in the outlet protein mixture at different protein concentrations (error bars extrapolated from standard deviations from total of 6 measurements). The percentage of avidin and BSA in the outlet was calculated based on equations given in the text

24.4%, respectively, and hence the percentage of avidin in the outlet was 14.9%, and that of BSA is 85.1% of the protein mixture. The results showed that BSA was significantly enriched in the outlet mixture compared to the initial 1:1 composition. Conversely, the captured proteins can be released by washing with high concentration salt solution, and enrichment of avidin can be achieved.

4 Conclusions

A novel nonfouling, functional surface coating based on HPGs was developed on PDMS surface as well in a PDMS-based microchannel. The carboxyl groups on the functionalized HPGs were used as a stationary support for the selective capture of positively charged proteins in PBS buffer at pH 7.4. The grafting process of HPGs onto the surface was followed using contact angle, ATR-FTIR, and EOF measurements. The new functional microfluidic device was tested to determine its ability to separate model proteins from a mixture. The capture of positively charged avidin was observed at various avidin–BSA mixture concentrations. In order to enhance the efficiency of the protein separation device, several essential parameters were identified and will need to be improved upon in future—these include increasing the surface-to-volume ratio of the PDMS column, optimizing the HPG graft density, grafting HPGs with higher numbers of carboxylic acid groups, and increasing the size (chain length) of the HPGs.

5 Supporting information available

Details of contact angle measurements of different surfaces treated with varying degrees of allylamine plasma treatment, of different molecular weight polymers, and of different grafting methods are available free of charge via the Internet at <http://www.springer.com/engineering/journal/10404>.

Acknowledgments Dr. Chiao is supported by Canada Research Chair, Tier 2 program and a discovery grant from the Natural Science and Engineering Research Council of Canada (NSERC). J.N.K. acknowledges the financial support from University of British Columbia, Canada Foundation for Innovation, and Michael Smith Foundation for Health Research. The authors thank the LMB Macromolecular Hub at the UBC Centre for Blood Research for the use of their research facilities. J.N.K is the recipient of a CBS/CIHR new investigator award in transfusion science, and N.A.A. Rossi is a recipient of a CBS/CIHR postdoctoral fellowship in Transfusion Science.

References

Ajikumar PK, Ng JK, Tang YC, Lee JY, Stephanopoulos G, Too HP (2007) Carboxyl-terminated dendrimer-coated bioactive interface for protein microarray: high-sensitivity detection of antigen in complex biological samples. *Langmuir* 23:5670–5677

- Barbosa JN, Madureira P, Barbosa MA, Aguas AP (2005) The influence of functional groups of self-assembled monolayers on fibrous capsule formation and cell recruitment. *J Biomed Mater Res A* 76:737–743
- Bi H, Meng S, Li Y, Guo K, Chen Y, Kong J, Yang P, Zhong W, Liu B (2006) Deposition of PEG onto PMMA microchannel surface to minimize nonspecific adsorption. *Lab Chip* 6:769–775
- Burns MA, Johnson BN, Brahmamandra SN, Handique K, Webster JR, Krishnan M, Sammarco TS, Man PM, Jones D, Heldsinger D, Mastrangelo CH, Burke DT (1998) An integrated nanoliter DNA analysis device. *Science* 282:484–487
- Chen Y, Tekmen M, Hillesheim L, Skinner J, Wu B, Müller JD (2005) Dual-color photon-counting histogram. *Biophys J* 88:2177–2192
- Cima LG (1994) Polymers for controlled biological interactions. *J Cell Biochem* 56:155–161
- de Malsche W, Eghbali H, Clicq D, Vangelooen J, Gardeniers H, Desmet G (2007) Pressure-driven reverse-phase liquid chromatography separations in ordered nonporous pillar array columns. *Anal Chem* 79:5915–5926
- de Vasconcelos CL, Bezerril PM, Dantas TNC, Pereira MR, Fonseca JLC (2007) Adsorption of bovine serum albumin on template-polymerized chitosan/poly(methacrylic acid) complexes. *Langmuir* 23:7687–7694
- Effenhauser CS, Bruin MGJ, Paulus A, Ehrat M (1997) Integrated capillary electrophoresis on flexible silicone microdevices: analysis of DNA restriction fragments and detection of single DNA molecules on microchips. *Anal Chem* 69:3451–3457
- Guo DJ, Han HM, Wang J, Xiao SJ, Dai ZD (2007) Surface-hydrophilic and protein-resistant silicone elastomers prepared by hydrosilylation of vinyl poly(ethylene glycol) on hydrosilanes-poly(dimethylsiloxane) surfaces. *Colloid Surf A* 308:129–135
- Harris JM (1992) Introduction to biotechnical and biomedical applications of poly(ethylene glycol). In: Harris JM (ed) *Poly(ethylene glycol) chemistry, biotechnical and biomedical applications*. Plenum Press, New York, pp 1–14
- He B, Tait N, Regnier F (1998) Fabrication of nanocolumns for liquid chromatography. *Anal Chem* 70:3790–3797
- Hu S, Ren X, Bachman M, Sims CE, Li GP, Allbritton N (2002) Surface modification of poly(dimethylsiloxane) microfluidic devices by ultraviolet polymer grafting. *Anal Chem* 74:4117–4123
- Huang B, Wu H, Kim S, Kobilka BK, Zare RN (2006) Phospholipid biotinylation of polydimethylsiloxane (PDMS) for protein immobilization. *Lab Chip* 6:369–373
- Kainthan RK, Gnanamani M, Ganguli M, Ghosh T, Brooks DE, Maiti S, Kizhakkedathu JN (2006a) Blood compatibility of novel water soluble hyperbranched polyglycerol-based multivalent cationic polymers and their interaction with DNA. *Biomaterials* 27:5377–5390
- Kainthan RK, Muliawan EB, Hatzikiriakos SG, Brooks DE (2006b) Synthesis, characterization, and viscoelastic properties of high molecular weight hyperbranched polyglycerols. *Macromolecules* 39:7708–7717
- Kainthan RK, Janzen J, Kizhakkedathu JN, Devine DV, Brooks DE (2008) Hydrophobically derivatized hyperbranched polyglycerol as a human serum albumin substitute. *Biomaterials* 29:1693–1704
- Kim P, Jeong HE, Khademhosseini A, Suh KY (2006) Fabrication of non-biofouling polyethylene glycol micro- and nanochannels by ultraviolet-assisted irreversible sealing. *Lab Chip* 6:1432–1437
- Lazar IM, Trisiripisal P, Sarvaiya HA (2006) Microfluidic liquid chromatography system for proteomic applications and biomarker screening. *Anal Chem* 78:5513–5524
- Liu J, Lee ML (2006) Permanent surface modification of polymeric capillary electrophoresis microchips for protein and peptide analysis. *Electrophoresis* 27:3533–3546

- Martins MCL, Fonseca C, Barbosa MA, Ratner BD (2003) Albumin adsorption on alkanethiols self-assembled monolayers on gold electrodes studied by chronopotentiometry. *Biomaterials* 24:3697–3706
- McNamee CE, Yamamoto S, Higashitani K (2007) Effect of the physicochemical properties of poly(ethylene glycol) brushes on their binding to cells. *Biophys J* 93:324–334
- Milner ST (1991) Polymer brushes. *Science* 251:905–914
- Mu L, Liu Y, Cai S, Kong J (2007) A smart surface in a microfluidic chip for controlled protein separation. *Chem Eur J* 13:5113–5120
- Muck A, Svatos A (2007) Chemical modification of polymeric microchip devices. *Talanta* 74:333–341
- Norde W, Buijs J, Lyklema H (2005) Adsorption of globular proteins. In: Lyklema H (ed) *Fundamentals of interface and colloid science*, vol V. London, Academic Press, pp 1–59
- Pathak S, Singh AK, McElhanon JR, Dentinger PM (2004) Dendrimer-activated surfaces for high density and high activity protein chip applications. *Langmuir* 20:6075–6079
- Prime KL, Whitesides GM (1993) Adsorption of proteins onto surfaces containing end-attached oligo(ethylene oxide): a model system using self-assembled monolayers. *J Am Chem Soc* 115:10714–10721
- Ramsey JD, Jacobson SC, Culbertson CT, Ramsey JM (2003) High-efficiency, two-dimensional separations of protein digests on microfluidic devices. *Anal Chem* 75:3758–3764
- Roberts MJ, Bentley MD, Harris JM (2002) Chemistry for peptide and protein PEGylation. *Adv Drug Deliv Rev* 54:459–476
- Rossi NAA, Kainthan RK, Scott MD, Brooks DE, Kizhakkedathu JN (2008) Surface grafting of polyglycerols to red blood cell membranes: Towards immunocamouflaged erythrocytes. *Polymer Prepr* 49:475–476
- Satulovsky J, Carignano MA, Szleifer I (2007) Kinetic and thermodynamic control of protein adsorption. *Proc Natl Acad Sci USA* 97:9037–9041
- Sharma S, Johnson RW, Desai TA (2003) Ultrathin poly(ethylene glycol) films for silicon-based microdevices. *Appl Surf Sci* 206:218–229
- Shimizu T, Yamoto M, Kikuchi A, Okano T (2001) Two-dimensional manipulation of cardiac myocyte sheets utilizing temperature-responsive culture dishes augments the pulsatile amplitude. *Tissue Eng* 7:141–151
- Singh N, Cui X, Boland T, Husson SM (2007) The role of independently variable grafting densities and layer thicknesses of polymer nanolayers on peptide adsorption and cell adhesion. *Biomaterials* 28:763–771
- Squires TM, Quake SR (2005) Microfluidics: fluid physics at the nanoliter scale. *Rev Mod Phys* 77:977–1026
- Stadler V, Beyer M, Koenig K, Nesterov A, Torralba G, Lindenstruth V, Hausmann M, Bischoff FR, Breitling F (2007) Multifunctional CMOS microchip coatings for protein and peptide arrays. *J Proteome Res* 6:3197–3202
- Tessmar JK, Göpferich AM (2007) Customized PEG-derived copolymers for tissue-engineering applications. *Macromol Biosci* 7:23–39
- Thongboonkerd V, Songtawee N, Sritippayawan S (2007) Urinary proteome profiling using microfluidic technology on a chip. *J Proteome Res* 6:2011–2018
- Thormanna W, Caslavská J, Mosher RA (2007) Modeling of electroosmotic and electrophoretic mobilization in capillary and microchip isoelectric focusing. *J Chromatogr A* 1155:154–163
- Wang R, Hashimoto K, Fujishima A, Chikuni M, Kojima E, Kitamura A, Shimohigoshi M, Watanabe T (1997) Light-induced amphiphilic surfaces. *Nature* 388:431–432
- Wang YC, Choi MH, Han J (2004) Two-dimensional protein separation with advanced sample and buffer isolation using microfluidic valves. *Anal Chem* 76:4426–4431
- Wang AJ, Xu JJ, Chen HY (2007) In situ grafting hydrophilic polymer on chitosan modified poly(dimethylsiloxane) microchip for separation of biomolecules. *J Chromatogr A* 1147:120–126
- Wu D, Zhao B, Dai Z, Qin J, Lin B (2006) Grafting epoxy-modified hydrophilic polymers onto poly(dimethylsiloxane) microfluidic chip to resist nonspecific protein adsorption. *Lab Chip* 6:942–947
- Xia Y, Whitesides GM (1998) Soft lithography. *Annu Rev Mater Sci* 28:153–184
- Xiao D, Zhang H, Wirth M (2002) Chemical modification of the surface of poly(dimethylsiloxane) by atom-transfer radical polymerization of acrylamide. *Langmuir* 18:9971–9976
- Xiao Y, Yu XD, Xu JJ, Chen HY (2007) Bulk-modification of PDMS microchips by amphiphilic copolymer. *Electrophoresis* 28:3302–3307
- Yao B, Luo GA, Feng X, Wang W, Chena LX, Wang YM (2004) A microfluidic device based on gravity and electric force driving for flow cytometry and fluorescence activated cell sorting. *Lab Chip* 4:603–607
- Yeh PYJ, Kainthan RK, Zou Y, Chiao M, Kizhakkedathu JN (2008) Self-assembled monothiol-terminated hyperbranched polyglycerols on a gold surface: a comparative study on the structure, morphology, and protein adsorption characteristics with linear poly(ethylene glycol). *Langmuir* 24:4907–4916
- Yu K, Han YC (2006) A stable PEO-tethered PDMS surface having controllable wetting property by a swelling–deswelling process. *Soft Matter* 2:705–709
- Zhang JG, Krajden OB, Kainthan RK, Kizhakkedathu JN, Constantinescu I, Brooks DE, Gyongyossy-Issa MIC (2008) Conjugation to hyperbranched polyglycerols improves RGD-mediated inhibition of platelet function in vitro. *Bioconjug Chem* 19:1241–1247